14 Derivation of Closure Relations and Commensurate State Variables for Meso-scale Models Using the REW Approach

ERWIN ZEHE, HAKSU LEE & MURUGESU SIVAPALAN

INTRODUCTION

Due to numerical reasons and data requirements, reasonable application of today's process based models such as MIKE SHE (Refsgaard & Storm, 1995), HYDRUS (Simunek *et al.*, 1994) or CATFLOW (Zehe *et al.*, 2001), is restricted to the hillslope and small catchment scales. Therefore, in spite of their shortcomings, conceptual hydrological models are nowadays still widely used for meso-scale modelling. Calibration used to be the "magical fix" to assess a model parameter set that optimally fits the target observations and compensates for all the unresolved spatial variability of input data, non-observable model parameters and state variables, as well as over-simplified process descriptions in conceptual models. However, as the optimal parameter sets are not unique (Beven, 1989; Beven & Freer, 2001) calibration has lost its magical touch and has become more and more a "quick fix" (Sivapalan *et al.*, 2003a), which may jeopardize the realism of the model. Due to the "equifinality" of optimal model parameter sets (Beven & Freer, 2001) and the missing link to catchment characteristics, conceptual model predictions are considerably uncertain when the model is used in a time period different from the calibration period, especially under changing boundary conditions, or in a similar catchment without re-calibration.

Parameter regionalization may be a way out of this crisis, as recently shown by, for example, Hundecha & Bárdossy (2004). The authors linked parameters of the HBV model to catchment characteristics in the Rhine basin using a transfer function approach, and derived behavioural parameter sets from catchment characteristics without re-calibration. However, if we do not stick to the usage of conceptual models the other more visionary way forward is to develop new process based hydrological models for meso-scale catchments. As suggested by Sivapalan *et al.* (2003a), the new generation of models should:

(a) be based on first principles, parameters and meaningful state variables which are, at least in principle, measurable in the field;
(b) represent the main effects of typical structures in a landscape on hydrological processes in different hydro-climates; and
(c) allow, therefore, better predictions with a minimum amount of necessary calibration.

The Representative Elementary Watershed (REW) approach (Reggiani *et al.*, 1998, 1999) offers a suitable framework for building such future hydrological models for the meso-scale. An REW is the smallest resolvable spatial unit within this modelling framework, delimited externally by a prismatic mantle, defined by the shape of the ridges circumscribing the sub-watershed. The REW is composed of an unsaturated zone, a saturated zone, a concentrated overland flow zone, a saturated overland flow zone and a channel zone. Within a thermodynamically consistent approach, Reggiani *et al.* (1998, 1999) derived a set of ordinary differential equations for mass, energy and momentum balance within the individual zones in the REW. Coupling between the balance equations is of course, as in the real world, due to fluxes that determine the exchange rates of water mass, energy and momentum between the different zones. Exchanges of water or heat between, for example, the soil and atmosphere or between the unsaturated and saturated zones, are determined by the spatial variability of surface and subsurface hydraulic and thermal properties. Subsurface structures especially, such as macropores/fractures or layers in the soil/aquifer, have a crucial influence. A major pre-requisite for applying the REW approach for modelling meso-scale watersheds is therefore to parameterize the effects of subscale surface and subsurface heterogeneities and structures within the "closure relations" that describe fluxes of water mass, momentum and energy between the different zones of an REW. In the following we refer to this problem as the closure problem.

We present an approach to assess closure relations for parameterizing the effect of typical subscale variabilities and structures inside a catchment/REW on the exchanges of water mass between different zones, by employing top-down as well as bottom-up arguments (Sivapalan *et al.*, 2003b). The test area is the Weiherbach catchment in the southwest of Germany. However, as Beven (2000) argues, each catchment is an "individual" due to individual details in subsurface structures, etc., and therefore the crucial question is: To what extent are these closure relations unique and only valid in the particular catchment they were derived for? Adopting the pattern-process paradigm and the idea of potential natural states from theoretical ecology (Watt, 1947; Turner, 1989; Turner & Gardner, 2001), we argue that it is possible to assess typical closure relations for specific landscapes and that these closure relations are transferable to different but similar catchments in the same landscape. The essence of the pattern-process paradigm is that similarity of patterns (e.g. in soils, vegetation and subsurface structures), in for example, two different catchments of a specific landscape, is an indicator of similarity of processes (Grayson & Blöschl, 2000; Underwood *et al.*, 2000). The potential natural state of a landscape is an equilibrium state due to a balance of "external" disturbances and "internal" forces. This balance is reflected in typical, spatially organized patterns of vegetation, soils and subsurface structures. Since these patterns had been formed by hydro-climatic processes in a specific geological environment, we argue that these typical patterns in a landscape in turn cause similarity of hydrological processes. We postulate, therefore, the existence of a typical process spectrum as a generic feature of a specific landscape, and therefore the existence of a set of typical closure relations for a specific landscape. We postulate, furthermore, that a meso-scale model based on the REW and landscape specific closure relations will likely require a minimum of calibration to account for the individual, unique structures in a specific catchment in that landscape.

In the present study we will demonstrate for the Weiherbach catchment, which is situated in a loess area in Germany, that:

(a) A process model which represents the typical spatial patterns of soils, vegetation and preferential pathways in that loess landscape is already sufficient to explain a large part of the observed hydrological processes, i.e. the dynamics of runoff, soil moisture and evapotranspiration (ET) within a long term simulation. We will call this model structure the landscape and process compatible one.
(b) By employing an averaging procedure described in the following section, the landscape and process compatible model allows derivation of closure relations for describing exchanges of water and momentum between the unsaturated and saturated zones. In particular we will show that model structures different from the landscape compatible one yield clearly different closure relations.
(c) The landscape compatible model allows derivation of catchment-scale state measures of average soil moisture and average capillary pressure that are consistent with subscale observations. These "commensurate" state measures may be used as additional target measures for validation of meso-scale models. In particular we will show that model structures different from the landscape compatible ones yield clearly different dynamics of catchment-scale state measures.

In the next section we briefly introduce the REW approach and the underlying theory for deriving closure relations and state measures by employing a distributed, physically based hydrological model named CATFLOW (Maurer, 1997; Zehe *et al.,* 2001). In the following two sections we will show that the proposed theory yields promising results for the intensively observed Weiherbach catchment in Germany. We close with a discussion of the results and an outlook on required future work.

THEORY

Outline of the REW Approach and the Closure Problem

The Representative Elementary Watershed approach has been proposed by Reggiani *et al.* (1998, 1999) as a thermodynamically consistent framework for deriving balance equations for hydrological modelling at the meso-scale. An REW is the smallest resolvable spatial unit of a meso-scale model, and is composed of five zones, which are the unsaturated zone (u-zone), saturated zone (s-zone), concentrated overland flow zone (c-zone), saturated overland flow zone (o-zone), and channel zone (r-zone). The mass, energy and momentum balances within the individual zones within the REW are described using a coupled set of ordinary differential equations, derived from thermodynamic principles by averaging. The volume making up a REW is delimited externally by the prismatic mantle, which is defined by the shape of the ridges circumscribing the sub-watershed. On top, the REW is delimited by the atmospheric boundary layer, and at the bottom by either an impermeable substratum or an assumed depth limit. The ensemble of REWs constituting the watershed interact with each other by way of exchanges of mass, momentum and energy through the inlet and outlet sections of the associated channel reaches (through the channel flow and backwater effects along the channel reaches), and laterally through the mantle separating REWs (e.g. through the exchange of groundwater and or thermal energy in the subsurface).

In the present study our focus is on the interactions between the different zones inside the REW due to the fluxes of water mass across the zonal boundaries. The governing mass balance equations for the five zones are given in equations (1) to (5) below. For the remaining balance equations for momentum and energy the reader is referred to Reggiani *et al.* (1998, 1999).

$$\frac{\mathrm{d}}{\mathrm{d}t}\left(\varepsilon y^s \omega^s\right) = \underbrace{e^{so}}_{\text{seepage}} + \underbrace{e^{su}}_{\text{exch. with unsat. zone}} + \underbrace{e^{sr}}_{\text{sat. zone - river exch.}} + \underbrace{\sum_I e_I^{sA} + e_{ext}^{sA}}_{\text{exch. across mantle segments}} \tag{1}$$

$$\frac{\mathrm{d}}{\mathrm{d}t}\left(\varepsilon y^u s^u \omega^u\right) = \underbrace{e^{uc}}_{\text{infiltration}} + \underbrace{e^{us}}_{\text{exch. with sat. zone}} + \underbrace{e_{wg}^{u}}_{\text{evaporation}} + \underbrace{\sum_I e_I^{uA} + e_{ext}^{uA}}_{\text{exch. across mantle segments}} \tag{2}$$

$$\frac{\mathrm{d}}{\mathrm{d}t}\left(y^c \omega^c\right) = \underbrace{e^{cu}}_{\text{infiltration into unsat. zone}} + \underbrace{e^{co}}_{\text{flow to sat. overl. flow}} + \underbrace{e^{ctop}}_{\text{rainfall or evaporation}} \tag{3}$$

$$\frac{\mathrm{d}}{\mathrm{d}t}\left(y^o \omega^o\right) = \underbrace{e^{or}}_{\text{lat. channel inflow}} + \underbrace{e^{os}}_{\text{seepage}} + \underbrace{e^{oc}}_{\text{inflow from conc. overl. flow}} + \underbrace{e^{otop}}_{\text{rainfall or evaporation}} \tag{4}$$

$$\underbrace{\frac{\mathrm{d}}{\mathrm{d}t}\left(m^r \xi^r\right)}_{\text{storage}} = \underbrace{e^{ro}}_{\text{lateral inflow}} + \underbrace{e^{rs}}_{\text{channel - sat.zone exch.}} + \underbrace{\sum_l e_l^{rA} + e_{ext}^{rA}}_{\text{inflow, outflow}} + \underbrace{e^{rtop}}_{\text{rainfall or evaporation}} \tag{5}$$

A necessary condition for the existence of a unique solution for any given set of equations is that the number of equations equals the number of unknowns. The e^{ij} terms in the mass balance equations (1) to (5) represent the mass exchange fluxes between the i and j sub-regions, are generally unknown, and must be externally specified. Closure of the set of model equations means, therefore, the derivation of:

(a) relations for describing exchanges of water mass between the different zones in the REW, and across the REW boundaries; and
(b) constitutive relations that link interdependent state variables, such as capillary pressure and saturation in the unsaturated zone.

As already discussed, appropriate closure relations must parameterize the effects of dominant sub-scale surface and subsurface heterogeneities on the fluxes of water mass. Following the pattern-process paradigm (Watt, 1947; Turner, 1989; Turner & Gardner, 2001), and as explained above, we postulate the existence of a generic spectrum of hydrological processes conditioned by the typical patterns of soils, vegetation and typical dominant structures in specific landscapes, and therefore the existence of a set of typical closure relations for a specific landscape. In the following sections we describe in detail how to derive such typical closure relations and how to estimate state measures that we call commensurate, based on the structure and the output of a spatially highly resolved process model.

Deriving commensurate, catchment-scale state measures using dynamical upscaling

A cardinal problem in hydrology is what we call the “scale gap” in understanding. We urgently need representative data on subsurface dynamics at the catchment scale, for

example, as additional performance measures for validating meso-scale models. However, due to the known shortcomings of geophysical measurement techniques such as time domain reflectometry (TDR) or ground penetrating radar (GPR), our observations, and therefore also our process understanding, are restricted to the point or small field scale. Common ways to assess information on the space–time pattern of soil moisture at larger scales is to perform a distributed set of point observations either using mobile sensors, such as the "green machine" (Western & Grayson, 1998), or a fixed set of TDR stations distributed in a catchment (Bárdossy & Lehman, 1995). The first approach is restricted to field campaigns and does not yield continuous information in time. The latter suffers from the fact that the correlation structure of soil moisture depends on the saturation state of the catchment (Grayson *et al.*, 1997). Hence, especially in dry states, the network might be too coarse for explaining spatial variability of soil moisture in a geo-statistical sense. Whatever measurement approach is employed, there is no easy way to scale the information from the distributed set of point observations to the catchment/REW scale because of nonlinear process dynamics and strong sub-catchment heterogeneity of soils and vegetation. Geostatistical interpolation, including updating approaches, suffer from the fact that they either assume stationary relations between drift parameters and soil moisture, or the sampling is not sufficient to obtain useful posterior probability distributions of soil moisture within different classes of available soft information. The basic idea of the approach presented here is to use a process model for dynamic upscaling:

(a) which explicitly represents the spatial patterns of soils, vegetation and preferential pathways inside a catchment, and the model is therefore landscape compatible;
(b) will be shown to portray the system's behaviour by comparing simulation results to a distributed set of observations of different state variables and fluxes such as soil moisture, discharge and evapotranspiration (ET), the model is therefore also process compatible.

Consequently, the fields of soil moisture $\theta(x,y,z,t)$ and matric potential $\psi(x,y,z,t)$ simulated by this model structure are landscape and process compatible, e.g. consistent with a distributed set of TDR observations. By integrating the model output over the total catchment volume and dividing by the catchment volume, we obtain time series of catchment-scale average soil moisture $\bar{\theta}(t)$ [L^3L^{-3}] and catchment-scale average matric potential $\bar{\psi}(t)$ [L], derived from this landscape and process compatible model structure:

$$\begin{aligned} \bar{\theta}(t) &= \frac{1}{V_{Catchment}} \iiint_{Catchment} \theta(x,y,z,t)\,\mathrm{d}x\,\mathrm{d}y\,\mathrm{d}z \\ \bar{\psi}(t) &= \frac{1}{V_{Catchment}} \iiint_{Catchment} \psi(x,y,z,t)\,\mathrm{d}x\,\mathrm{d}y\,\mathrm{d}z \end{aligned} \tag{6}$$

where x, y, z denote the Cartesian coordinates and t the time.

In the following sections this dynamical upscaling will be exemplified for the Weiherbach catchment by employing a landscape compatible model structure based on the process model CATFLOW (Mauer, 1997; Zehe *et al.*, 2001). The model is also process compatible as it yields simulation results in good agreement with TDR measurements at 61 locations, discharge observations as well as observed ET. We consider the state measures derived from the landscape and process compatible model

structure using equation (7) as physically consistent with the local observations, and refer to them as commensurate state measures. Consequently, we postulate that the time series of catchment-scale average soil moisture and matric potential may be used as additional target measure for validation of meso-scale models in this area. In particular, we will show that model structures different from the landscape and process compatible one yield clearly different dynamics of the catchment-scale average soil moisture and matric potential.

Deriving closure relations at the REW scale using fine scale process models

If we assume no exchanges between neighbouring REWs the mass balance equation, equation (2), for the unsaturated zone reduces to:

$$\frac{\mathrm{d}}{\mathrm{d}t}\left(\rho\varepsilon y^u s^u \omega^u\right) = \underbrace{e^{uA}}_{\text{evapotranspiration}} + \underbrace{e^{us}}_{\text{percolation}} + \underbrace{e^{uc}}_{\text{infiltration}} \tag{7}$$

where y^u [L] is the average thickness of the unsaturated zone, s^u [–] is the average saturation, ω^u [L^2] is the total catchment area of the unsaturated zone, ε^u [L^3L^{-3}] is the porosity and ρ [ML^{-3}] is the mass density of water; e^{uA}, e^{us}, e^{uc} denote the mass exchange rates at the interface to the atmosphere, saturated zone and concentrated overland flow zone, respectively.

We focus on the exchange terms e^{uc} and e^{us}, which denote infiltration from the concentrated overland flow zone into the unsaturated zone, as well as percolation into groundwater. The most fundamental assumption we make is that capillary forces and gravity are still the major drivers for infiltration and percolation at the REW scale. Hence, we assume that water fluxes e^{uc} and e^{us} are still driven by average gradients of matric potential and gravity, that catchment-scale average water saturation in the unsaturated zone is related to catchment-scale average capillary pressure $\overline{\psi}$ by an average water retention function, and that average flow resistance may be described by an average catchment-scale hydraulic conductivity curve k^*:

$$\begin{aligned} e^{cu} &= -k^*\left(S^u\right)\left.\frac{\partial\overline{\psi}}{\partial z}\right|_{cu} - k^*\left(S^u\right) \\ e^{us} &= -k^*\left(S^u\right)\left.\frac{\partial\overline{\psi}}{\partial z}\right|_{us} - k^*\left(S^u\right) \\ \overline{\psi} &= f(S^u) \end{aligned} \tag{8}$$

The basic idea is now to derive k^* and $\overline{\psi} = f(S^u)$ as well as the average catchment-scale hydraulic conductivity curve from the parameter structure, and the output of a model that was shown to be landscape and process compatible in the sense specified above. Using perturbation analysis (Duffy 1996; Dagan, 1986), and the ergodic assumption, we divide the field of unsaturated hydraulic conductivity k and the field of matric potential ψ, which are parameters and output of the landscape and process compatible model structure, into catchment-scale spatial average $\overline{\psi}$, $\overline{k}$, and subscale deviations ψ', k' with zero spatial average at a fixed time:

$$\begin{aligned} k(x,y,z,\theta(x,y,z,t)) &= \overline{k}(\theta(x,y,z,t)) + k'(x,y,z,\theta(x,y,z,t)) \\ \psi(x,y,z,t) &= \overline{\psi}(t) + \psi'(x,y,z,t) \end{aligned} \tag{9}$$

Inserting definition (equation (9)) into the usual Darcy's law (equation (10)), and spatial averaging, yields equation (11) for the catchment/REW scale vertical water flux in the unsaturated zone $\bar{q}$ [LT^{-1}]:

$$q(x,y,z,t) = k(x,y,z,\theta(x,y,z,t))\frac{\partial(\psi(x,y,z,t)+z)}{\partial z} \tag{10}$$

$$\bar{q}(t) = \left[\overline{k(\theta)} + \frac{\overline{k'(x,y,z,\theta(x,y,z,t))\frac{\partial(\psi'(x,y,z,t)+z)}{\partial z}}}{\frac{\partial(\bar{\psi}(t)+z)}{\partial z}}\right]\frac{\partial\bar{\psi}(t)+z}{\partial z} \cong k^*(\bar{\theta})\left(\overline{\frac{\partial\psi(t)}{\partial z}}+1\right) \tag{11}$$

In the last step in equation (11) the vertical gradient of the average catchment-scale matric potential was approximated by the catchment-scale average of the vertical gradients, which may be calculated from the model output. If we define the average catchment-scale hydraulic conductivity k^* according to equation (12), we may compute k^* at each time step directly from the model output and the known spatial patterns of unsaturated hydraulic conductivity, which represents the typical spatial patterns of soils and macropores in the catchment:

$$\overline{k(\theta(x,y,z,t))} + \frac{\overline{k'(x,y,z,\theta(x,y,z,t))\frac{\partial(\psi'(x,y,z,t)+z)}{\partial z}}}{\overline{\frac{\partial\psi(t)}{\partial z}}+1} \equiv k^*(\overline{\theta(t)}) \tag{12}$$

The properties on the left hand side of equation (12) may be derived from the parameter fields of the landscape and process compatible model structure. The second order term denotes the spatial covariance between the unsaturated hydraulic conductivity and the vertical matric potential gradient. Intuitively we expect this term to be zero, when there is random variability of soils inside the catchment. However, it might be non-zero if there is structured variability of soils inside the catchment, because soil unsaturated hydraulic conductivity and soil water retention properties are not independent.

Assuming the parametric relationships for the catchment-scale water retention curve and catchment-scale hydraulic conductivity as functions of catchment-scale water saturation in the unsaturated zone given by equation (13) below, we may derive the required constitutive relations using the landscape and process compatible model structure for simulating catchment-scale drainage and wetting experiments:

$$\begin{aligned} k^*(S^u) &= \bar{k}_s\left(\frac{\bar{\theta}}{\bar{\theta}_s}\right)^{\beta} \\ \bar{\psi}(S^u) &= \left(\frac{\bar{\theta}}{\bar{\theta}_s}\right)^{\alpha} \\ S^u &= \frac{\bar{\theta}}{\bar{\theta}_s} \end{aligned} \tag{13}$$

As k^*, the average saturated hydraulic $\bar{k}_s$ and porosity $\bar{\theta}_s$ as well as $\bar{\theta}$ may be derived from the model structure and the model output (using equation (7)), the parameters α

and β maybe determined by plotting the left hand side against the right hand side in equation (13) and fitting a potential law. This method of deriving closure relations for mass exchange will be exemplified later for the Weiherbach catchment. In particular we will show that model structures different from the landscape compatible and process compatible one yield clearly different values for α and β.

APPLICATION TO A TYPICAL CATCHMENT IN A LOESS AREA

Study Area and Database

1. Characteristics, typical structures and runoff generation

The application of the proposed theory is based on detailed laboratory data and field observations that were conducted in the Weiherbach valley (Zehe *et al.*, 2001). The Weiherbach is a rural catchment of 3.6 km^2 size situated in a loess area in the south-west of Germany. Geologically it consists of Keuper and loess layers of up to 15 m thickness. The climate is semihumid with an average annual precipitation of 750–800 mm $year^{-1}$, average annual runoff of 150 mm $year^{-1}$, and annual potential evapo-transpiration of 775 mm $year^{-1}$.

More than 95% of the total catchment area is used for cultivation of agricultural crops or pasture, 4% is forested and 1% is paved area. Crop rotation is usually once a year. Typical main crops are barley or winter barley, corn, sunflowers, turnips and peas; typical intermediate crops are mustard or clover. Ploughing is usually to a depth of 30 to 35 cm in early spring or early autumn, depending on the cultivated crop. A few locations in the valley floor are tile drained to a depth of about 1 m. However, the total portion of catchment area that is under tile drains is less than 0.5% of the total catchment.

Most of the Weiherbach hillslopes exhibit a typical loess catena with moist but drained colluvisols located at the foothills and dryer calcaric regosols located at the top and mid-slope sectors. Preferential pathways in the Weiherbach soils are very apparent. They are mainly a result of earthworm burrows and their spatial pattern is closely related to the typical hillslope soil catena (Ehrmann, 1996; Zehe & Flühler, 2001). The preferential pathways, or macropores, enhance infiltration and decrease storm runoff as storm runoff only consists of surface runoff in this type of landscape.

The detailed field observations (Zehe *et al.*, 2001) in the Weiherbach catchment indicated that storm runoff is produced by infiltration excess overland flow. Due to the small portion of tile-drained areas, runoff from tile drains is of minor importance for catchment-scale runoff response. Any water that infiltrates into the soil percolates into the deep loess layer. A bromide tracer experiment conducted over two years on an entire hillslope in the catchment suggested that there is very little lateral flow in the soils (Delbrück, 1998). There is an aquifer at the base of the loess layer. The tracer experiment also indicated that the travel time for the infiltrating water to reach the aquifer is likely to be more than 10 years. As a result of these mechanisms, event runoff coefficients are small. The runoff coefficient for the largest event in the record of 15 years was 0.13, for the second largest event it was 0.07, and runoff coefficients for the remainder of the storms are of the order 0.01.

2. Experimental database

Figure 14.1 (right panel) gives an overview of the observational network in the northern part of Weiherbach catchment. Rainfall input was measured at a total of six

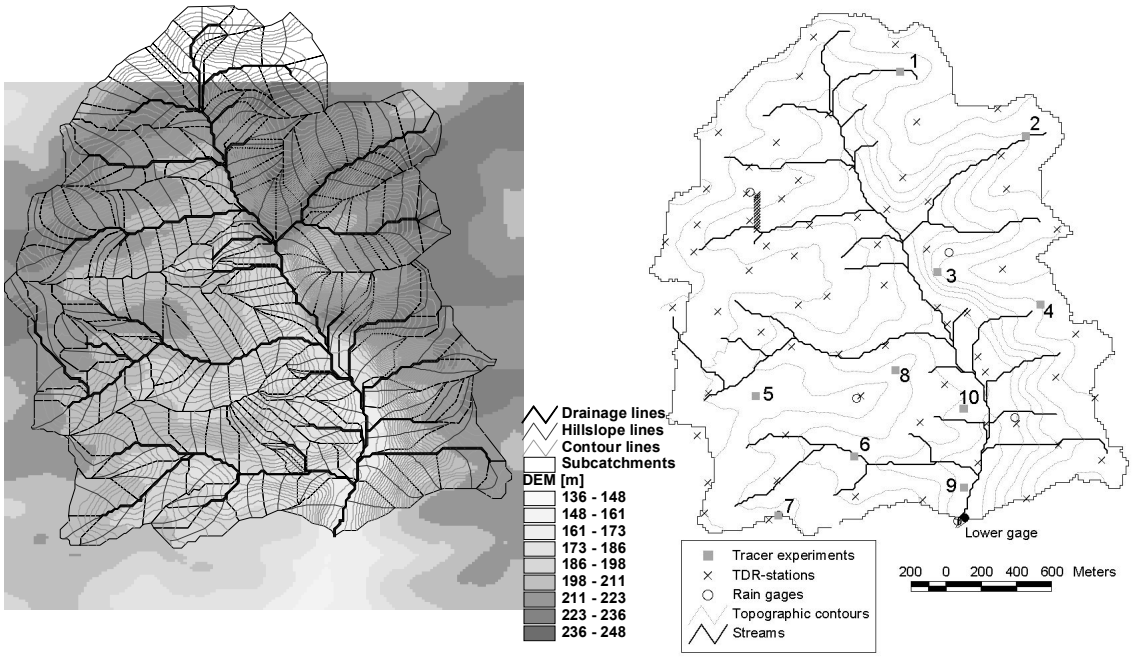

Fig. 14.1 *Observational network of the Weiherbach catchment (right panel). Soil moisture was measured at 61 TDR stations at weekly intervals (crosses). The triangle indicates the streamgauge. The topographic contour interval is 10 m. The left panel shows the subdivision of the catchment according to hill slope and the related drainage network, as well as the gridded elevation.*

Table 14.1 *Laboratory measurements of average hydraulic properties for typical Weiherbach soils. Definition of parameters after van Genuchten (1980) and Mualem (1976). Saturated hydraulic conductivity k_s, porosity θ_s, residual water content θ_r, air entry value α, shape parameter n.*

	k_s (m s^{-1})	θ_s (m^3 m^{-3})	θ_r (m^3 m^{-3})	α (m^{-1})	n (–)
Calcaric regosols	2.1×10^{-6}	0.44	0.06	0.40	2.06
Colluvisols	5.0×10^{-6}	0.40	0.04	1.90	1.25
Sand	8.25×10^{-5}	0.43	0.034	14.50	2.68

raingauges and streamflow was monitored at two streamgauges, all at a temporal resolution of 6 minutes. The gauged catchment areas are 0.32 and 3.6 km^2. Soil moisture was measured at up to 61 locations at weekly intervals using two-rod TDR equipment that integrates over the upper 15 cm of the soil. As the total area is 3.6 km^2, the 61 measurement points used effectively translates to an average spacing of 250 m (Western & Blöschl, 1999). The soil hydraulic properties of typical Weiherbach soils, after van Genuchten (1980) and Mualem (1976), were measured in the laboratory using undisturbed soil samples taken along transects at several hillslopes, up to 200 samples per slope (Table 14.1; Schäfer, 1999).

A soil map was compiled from texture information that was available on a regular grid of 50 m spacing. The macropore system was mapped at 15 sites in the catchment; each 1-m^2 large plot was subdivided into 0.5 m^2 raster elements and a horizontal soil profile was prepared. For each element, macropores that were connected to the soil

surface were counted and their depth and diameter were measured using a vernier calliper and a wire. The topography was represented by a digital elevation model of 12.5 m grid spacing. Curves for the temporal development of LAI, plant height, biomass production, and root length were determined based on visual inspections of the main crops such as corn, wheat, oats, sun flowers, sugar beets, peas, mustard and turnips as bases for the evaporation module of CATFLOW. Further details on the measurement program are given in Zehe *et al.* (2001).

As expected for this loess area, the catchment-scale pattern of soil types turned out to be highly organized. The typical loess soil catena on a hillslope is calcaric regosols at the top and mid-slope sector, and colluvisols in the valleys. The spatial patterns of the macropore characteristics observed in the Weiherbach catchment are closely related to the soil catena. The macroporosities tend to be small in the dry calcaric regosols located at the top and mid-slope, and larger in the moist and drained colluvisols located on the foot-slopes (Zehe, 1999; Zehe & Flühler, 2001). The observations at the 15 sites were used to choose a simple pattern of macroporosity for the catchment-scale simulations. The number of worm burrows connected to the soil surface turned out to vary throughout the year. Macropores that link the plough horizon and the subsoil are partly destroyed (Flury, 1996) through ploughing in spring and rebuilt by the earth-worms in summer and early autumn. Therefore, the number of macropores that connect top and subsoil appears to peak in late summer or early autumn. As this spatially organized pattern of soils and macropores represents a potential natural state of this landscape, even after moderate disturbances the landscape relaxes back to this equilibrium state due to positive feedback.

The Process Model CATFLOW

Model simulations were performed using a physically based model named CATFLOW (Maurer, 1997; Zehe *et al.,* 2001). The model subdivides a catchment into a number of hillslopes and a drainage network. Each hillslope is discretized along the main slope line into a two-dimensional vertical grid using curvilinear orthogonal coordinates. Each model element, as defined by the grid, extends over the width of the hillslope. The widths of the elements vary from the top to the foot of the hillslope. For each hillslope, evapotranspiration E_{act} [LT^{-1}] is represented using an advanced SVAT approach based on the Penman-Monteith equation, which accounts for plant growth, albedo as a function of soil moisture and the impact of local topography on wind speed and radiation:

$$E_{act} = \frac{1}{\lambda}\left[\frac{\Delta(R_n - G) + \rho c_p \left(e_s - e_a\right)/r_a}{\Delta + \gamma\left(1 + r_x/r_a\right)}\right] \tag{14}$$

where λ [$M L^2 T^2$] is the specific heat of evaporation, Δ the slope of the vapour pressure curve, γ the psychrometric constant, R_n is global radiation, G soil heat flux, r_x turbulent resistance of canopy or soil, and r_a turbulent atmospheric resistance.

Soil water dynamics and solute transport are simulated based on the Richards equation in the mixed form as well as a transport equation of the convection diffusion type.

$$\frac{\partial \theta}{\partial \psi}\frac{\partial \psi}{\partial t} = \nabla\left(\underbrace{k\ (\theta)\nabla(\psi + z)}_{\mathbf{q}}\right)$$
$$R\frac{\partial C_w}{\partial t} = -\nabla(vC_w) + \nabla(D_e \nabla C_w) + s_a \tag{15}$$

C_w [ML^{-3}] is the residual concentration in the water phase, R [–] the retardation coefficient, v [LT^{-1}] the pore water velocity, and D_e [L^2T^{-1}] the effective dispersion coefficient. Soil hydraulic functions are parameterized after van Genuchten (1980) and Mualem (1976).

An implicit mass conservative "Picard iteration" (Celia & Bouloutas, 1990) and a random walk (particle tracking) scheme, are used to solve equation (15) numerically. The simulation time step is dynamically adjusted to achieve an optimal change of the simulated soil moisture per time step, which assures fast convergence of the Picard iteration.

The hillslope module of CATFLOW can simulate infiltration excess runoff, saturation excess runoff, re-infiltration of surface runoff, lateral water flow in the subsurface, return flow and solute transport. However, in the Weiherbach catchment only infiltration excess runoff contributes to storm runoff and lateral subsurface flow does not play a significant role at the event scale. What is important is the redistribution of near-surface soil moisture in controlling infiltration and surface runoff. As the portion of the tile-drained area in the catchment is smaller than 0.5%, we did not account for tile drains in the simulations.

Surface runoff is routed down the hillslopes, fed into the channel network and routed to the catchment outlet based on the diffusion wave approximation to the one dimensional Saint-Venant equations given below:

$$\frac{\partial h}{\partial t} + \frac{1}{b_w}\frac{\partial Q}{\partial y} = \frac{1}{b_w}\frac{\partial Q_{lat}}{\partial y}$$
$$\frac{\partial Q}{\partial t} + \frac{\partial}{\partial y}\left(\frac{Q^2}{A}\right) + \left(qA\frac{\partial h}{\partial y} + \frac{Q|Q|}{K_Q^2} - I_S\right) = 0 \tag{16}$$
$$K_Q = \frac{1}{n_m}A^{5/3}U^{2/3}$$

where h is the water depth, Q the discharge, Q_{lat} the lateral inflow from hillslope elements, b_w is the channel width at the water surface, A the cross sectional area, U the wetted perimeter, and n_m the Manning-Strickler coefficient.

As preferential flow and transport are important in the Weiherbach catchment, their representation is described in some detail below. Preferential flow and transport are represented by a simplified, effective approach similar to the 1-D approach of Zurmühl & Durner (1996). However, while Zurmühl & Durner (1996) used a bimodal function to account for high unsaturated conductivities at high water saturation values, we use a threshold value S_0 for the relative saturation S [–], which is motivated by the experimental findings of Zehe & Flühler (2001). If S at a macroporous grid point at the

soil surface exceeds this threshold, the bulk hydraulic conductivity, k^B, at this point is assumed to increase linearly as follows:

$$k^B(x,z) = k_S(x,z) + k_S(x,z) f_m(x,z) \frac{S - S_0}{1 - S_0} \quad if\ S \geq S_0$$
$$k^B(x,z) = k_S(x,z) \qquad \text{otherwise} \qquad (17)$$
$$S(x,z) = \frac{\theta(x,z) - \theta_r(x,z)}{\theta_s(x,z) - \theta_r(x,z)}$$

where k_s [L T^{-1}] is the saturated hydraulic conductivity of the soil matrix, θ_s [L^3 L^{-3}] and θ_r [L^3 L^{-3}] are saturated and residual soil moisture, respectively, x and z are the coordinates along the slope line and the vertical.

The macroporosity factor, f_m [–], is defined as the ratio of the water flow rate in the macropores Q_m [L^3 T^{-1}] in a model element of area A, and the saturated water flow rate in the soil matrix Q_{matrix} [L^3 T^{-1}]. It is therefore a characteristic soil property reflecting the maximum influence of active preferential pathways on saturated soil water movement:

$$f_m(x,z) = \frac{Q_m(x,z)}{Q_{matrix}(x,z)} \qquad (18)$$

where Q_{matrix} and Q_m are the water flow rates in the matrix and the macropores, respectively.

In our simulations we chose the threshold S_0 to equal 0.8, which corresponds to a soil moisture value of 0.32 in the colluvisols. This is a plausible value as it is of the order of the field capacity for the soils in the Weiherbach catchment. It is likely that for relative saturation values above this threshold, free gravity water is present in the coarse pores of the soil, and this free water may percolate into macropores and start preferential flow.

Internal Model Tests

1. Flow and transport at the plot and hillslope scale

Using the hillslope module of CATFLOW, Zehe & Blöschl (2004) simulated preferential flow and tracer transport at several field plots in the Weiherbach catchment in accordance with observations. The two dimensional f_m pattern in the macroporous medium they used for their study was computed using equation (17) based on a statistical generation of macropores of different sizes, and assigning macropore flow rates to each macropore, which were measured using macroporous soil samples (Zehe & Flühler, 2001). Furthermore, simulations of tracer transport and water dynamics over an entire hillslope over a period of two years matched the corresponding observations of a long-term tracer experiment at the hillslope scale well (Zehe *et al.*, 2001). For reasons of brevity the corresponding graphs are not presented here, but interested readers are referred to Zehe *et al.* (2001) and Zehe & Blöschl (2004). We therefore believe that this threshold approach and the selected threshold of $S_0 = 0.8$ is suitable to represent the important effects of macropores and their spatial patterns on infiltration and runoff generation in the Weiherbach catchment and more generally in this loess area.

2. Catchment-scale model setup and parameter estimation

Model set-up For the catchment-scale simulations, the Weiherbach catchment was subdivided into 169 hillslopes and an associated drainage channel network; the surface model elements can be seen in Fig. 14.1 (left panel). The hillslope model elements, typically, are 5–20 m wide (depending on the position on the hillslope), 10 m long, and the depth of each element varies from 5 cm for the surface elements to 25 cm for the lower elements. The total soil depth represented by the model was 2 m. The Manning roughness coefficients for the hillslopes and the channels were taken from a number of irrigation experiments performed in the catchment, as well as from the literature, based on the current crop pattern (see Gerlinger *et al.*, 1998; Zehe *et al.*, 2001). For the hillslopes the following boundary conditions were chosen: free drainage at the bottom, seepage boundary conditions at the interface to the stream, atmospheric conditions at the upper boundary, no flux boundary at the watershed boundary.

Because of the spatially highly organized hillslope soil catena observed, which is typical of hillslopes in this landscape, all hillslopes in the model catchment were given the same relative catena with calcaric regosols on the upper 80% and colluvisols on the lower 20% of the hillslope. The corresponding van Genuchten-Mualem parameters are listed in Table 14.1. The measurements of macroporosity at 15 sites in the Weiherbach catchment suggested high values in the moist colluvisols on the foot-slopes and low values at the top and mid-slope sectors. At the foot of the hillslopes the macropore volumes typically were 1.5×10^{-3} m^3 for 1 m^2 sampling area, while at the top they typically were 0.6×10^{-3} m^3 (see Fig. 4.1 of Zehe, 1999). The most parsimonious approach that accounts for this structured variability is what we call a "deterministic pattern" of the macroporosity factor with scaled values of the macroporosity factor in each hillslope. We chose the macroporosity factor to be $0.6 \times f_m$ for the upper 70% of the hillslope, $1.1 \times f_m$ over the mid-sector ranging from 70% to 85 % of the hillslope, and $1.5 \times f_m$ in the lowest 85% to 100 % of the slope length, where f_m is the average macroporosity factor of the hillslopes. The depth of the macroporous layer was assumed to be constant throughout the whole catchment and was set at 0.5 m. The only remaining free parameter is the average macroporosity factor f_m of the hillslopes. As the number of macropores connected to the soil surface varies throughout the year, the f_m value has to be calibrated when we focus on the event scale.

Model calibration and sensitivity for average macroporosity We calibrated the catchment-scale model by adjusting the macroporosity factor for the two largest observed rainfall–runoff events on record observed on the 27 June 1994 and 13 August 1995 (Table 14.2). The initial states were estimated based on 61 soil moisture observations using Simple Updating Kriging, and the amount of fine pores in the soil estimated from the texture classes (Zehe & Blöschl, 2004). For rainfall event #1 (June 1994) we found an optimum macroporosity factor of $f_m = 2.1$, which corresponds to the hydrograph with crosses in Fig. 14.2 (bottom left panel). Furthermore, the bottom left panel of Fig. 14.2 shows the simulated hydrographs for f_m values ranging from 0 to 3 to illustrate the strong dependence upon macroporosity. The rainfall events #1 (June 1994) and #2 (August 1995) are very similar in terms of their magnitudes, average intensities (Table 14.2) and initial soil moistures. However, the corresponding event runoff coefficients calculated from the observed hydrographs differ by a factor of almost 2 (Table 14.2). Apparently, the infiltration capacity of the soil was higher in

Table 14.2 *Measured characteristics of the two largest rainfall–runoff events on record: precipitation depth P, average precipitation intensity I, peak discharge at the catchment outlet Q_{max}, event runoff coefficient C, average initial soil moisture $\bar{\theta}$ and spatial variance Var_θ, number of available TDR observations in space N_{obs}. Weiherbach lower gage, 3.6 km² catchment area.*

Event	Date	P (mm)	I (mm h^{-1})	Q_{max} (m^3 s^{-1})	C (–)	$\bar{\theta}$ (–)	Var_θ (–)	N_{obs}
#1	27 June 1994	78.3	22	7.9	0.12	0.25	0.32	61
#2	13 August 1995	73.2	23	3.2	0.07	0.26	0.41	57

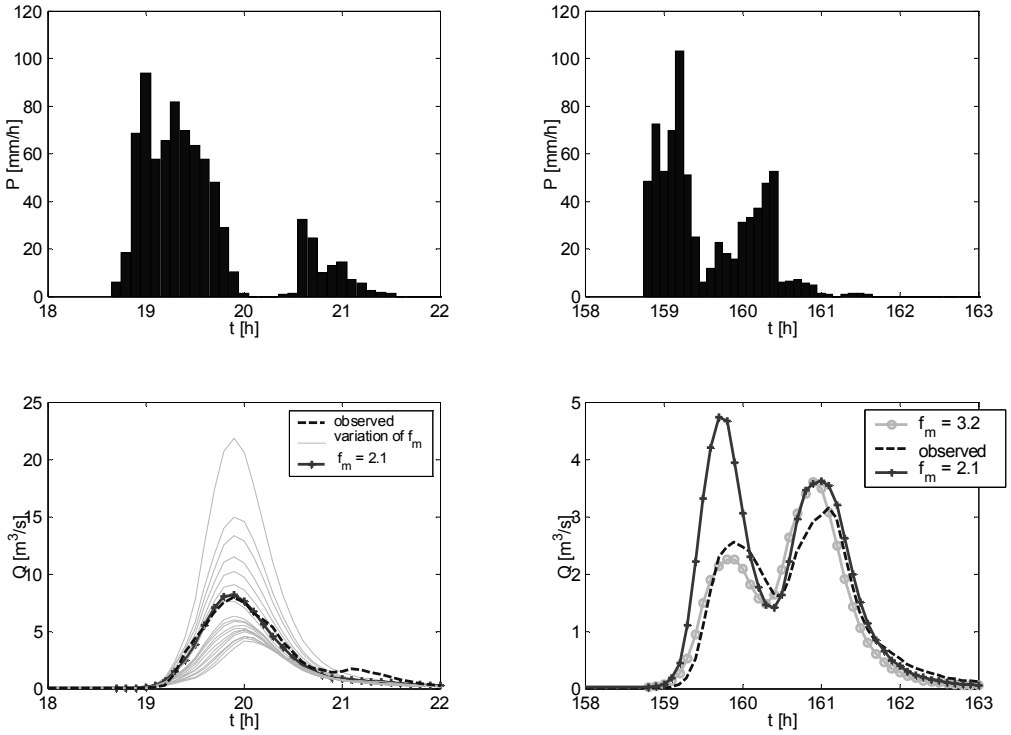

Fig. 14.2 *Lower left panel: Simulated discharges (thin solid lines) for event #1 (June 1994) for macroporosity factors ranging from f_m = 0 to 3. Increasing values of f_m correspond to decreasing runoff. The best fit to the observed hydrograph is obtained for f_m = 2.1 (crosses). Lower right panel: Event #2 (August 1995), simulation with f_m = 2.1 (crosses) and best fit with f_m = 3.2 (circles). The upper two panels show the corresponding precipitation in the Weiherbach catchment (3.6 km²).*

August 1995 than it was in June 1994. A possible explanation is a reduced infiltration capacity of the surface in June 1994 due to erosion and surface siltation. Another likely explanation is a seasonal variation of the number of macropores (i.e. earthworm burrows) that connected the soil surface and the subsoil below the plough horizon. This interpretation is consistent with the findings of several authors discussed in a review by Flury (1996, pp. 34–36) on the transport of pesticides in the soil. Flury noted that continuous macropores are disrupted by ploughing, e.g. in spring, and reconnected to the soil surface by earthworm activity during summer. A reduced depth of macropores leads to reduced infiltration as shown by Mauer (1997) and Bronstert & Plate (1997).

For an accurate simulation of event #2 we had to increase the f_m value to 3.2 (Fig. 14.2, bottom right panel). During a continuous simulation it is very difficult to account for non-stationarity of infiltration characteristics due to surface siltation or variations in macroporosity. We therefore used an average macroporosity of f_m = 2.1 during a continuous simulation of 1.5 years.

3. Continuous catchment-scale model test

Based on the typical model structure outlined above, the water cycle in the Weiherbach catchment was continuously simulated for the period 21 April 1994 to 15 September 1995. During simulation we accounted for plant growth and related changes in LAI, plant height and root depth as well as for seasonal changes in the crop pattern. Meteorological input data were taken from the meteorological station in the centre of the catchment, wind speed and radiation were regionalized to the catchment scale, as described in Zehe *et al.* (2001). After an initialization phase of approximately 30 days the model yields, simultaneously, reasonable predictions of discharge with a Nash-Sutcliffe efficiency of 0.82, and good predictions of evapotranspiration (ET) with a correlation of R = 0.91 (Fig. 14.3). Furthermore, the model yields reasonable predictions of soil moisture dynamics at 61 sites within the catchment, as shown for sites at the hilltop (Fig. 14.4 upper 9 panels) and bottom slope sectors (Fig. 14.4 lower panels), presented here as examples. The average correlation between observed and simulated soil moisture was 0.64 at hilltop locations and 0.74 at the mid-slope and valley floor sectors.

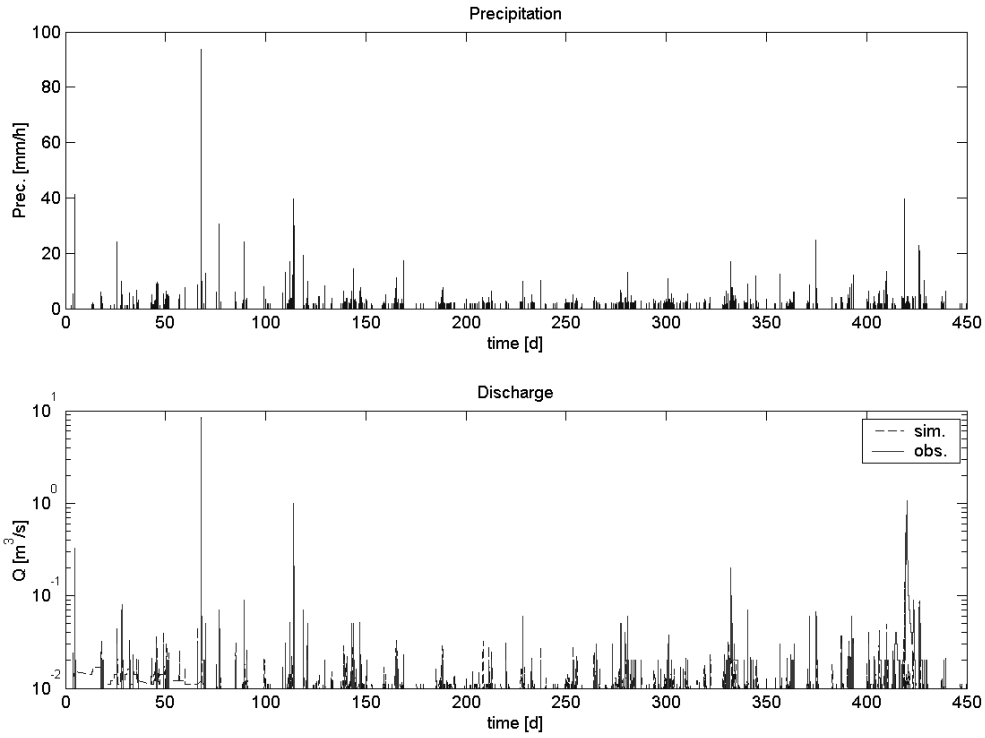

Fig. 14.3 *Precipitation, and simulated and observed discharge at the catchment outlet for 21 April 1994 to 15 September 1995; the Nash Sutcliffe coefficient is 0.82.*

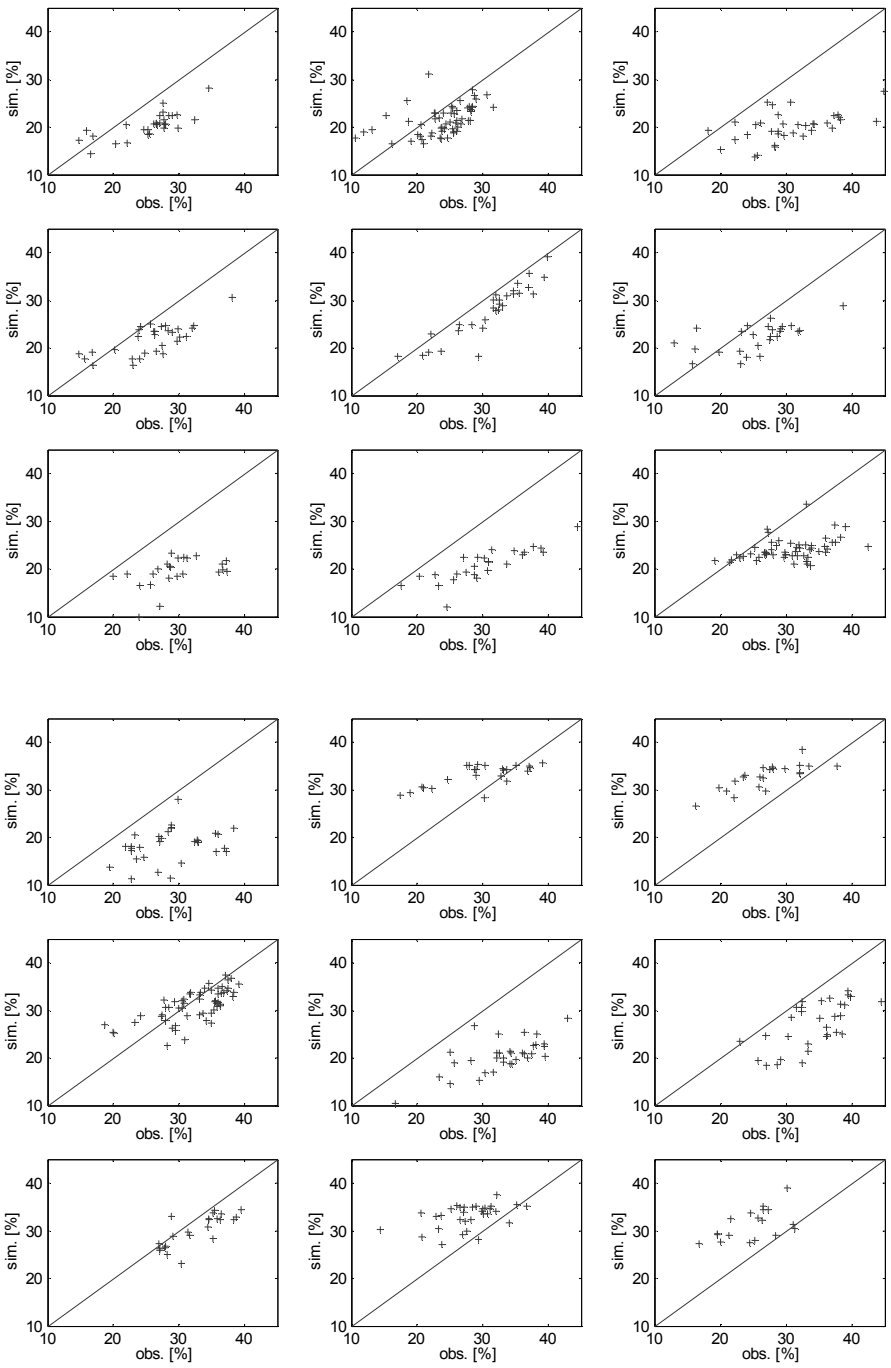

Fig. 14.4 *Simulated and observed soil moisture. Examples shown for 9 TDR stations located at hill tops (upper 9 panels) and 9 TDR stations located on the valley floor (lower 9 panels). Correlation was, on average 0.64, at hill top and 0.74 at mid slope and valley floor. Note that the model does not account for deviations from the idealized hillslope soil catena.*

The reader should keep in mind that the model structure only accounts for typical variability exhibited in the catchment, i.e. the idealized hillslope soil catena and the related structured pattern of macroporosity outlined in the previous section. Small-scale variability of soil hydraulic properties as well as palaeo-soils, which also occurs at some locations in the Weiherbach catchment, has been neglected. Nevertheless, a major part of the variability of soil moisture, discharge and *ET* may already be explained by the model.

DERIVATION OF CLOSURE RELATIONS AND COMMENSURATE STATE VARIABLES

Time Series of Average Catchment-scale Soil Moisture and Capillary Pressure

In the last section we introduced the process model CATFLOW, and demonstrated that a model structure that represents the dominant spatial pattern of soil and macroporosity, without accounting for small-scale details, is nevertheless sufficient for predicting discharge, *ET* and up to 60% of soil moisture dynamics observed at 61 distributed locations in the catchment. This model structure is therefore landscape and process compatible. The simulated distributed fields of soil moisture and capillary pressure are landscape and process compatible too, i.e. physically consistent with a distributed set of observations inside the catchment. The corresponding time series of catchment-scale average soil moisture and capillary pressure, computed using equation (6), are what we call commensurate state measures, as they are derived from a landscape and process compatible model structure by means of averaging.

In this section we will show that model structures, which even slightly differ from the landscape and process compatible one, yield different predictions of streamflow, hence they are not process compatible. Comparison between time series of catchment-scale average soil moisture and matric potential derived from different model structures will shed light on the question whether the differences in soil moisture within the catchment vanish if we move to the catchment scale. To this end we compared the following model structures during a simulation covering the period from the 21 April 1994 to 15 September 1995:

- Landscape and process compatible model structure This is the structure that yielded the predictions presented in the section above, i.e. calcaric regosols in the upper 80% and colluvisols in the lower 20% of the hillslope (see Table 14.1 for the soil hydraulic parameters), deterministic macroporosity pattern with 0.6 f_m at the upper 70% of the hillslope, $1.1 \times f_m$ at the mid sector ranging from 70–85% of the hillslope, and $1.5 \times f_m$ at the lowest 85–100%, average macroporosity value was $f_m = 2.1$.
- No macropores Using the same soil pattern as in the landscape and process compatible model structure above, but neglecting the macropores.
- Disturbed macroporosity Using the same soil pattern as in the landscape and process compatible model structure as above, but the macroporosity pattern was flipped, i.e. $0.6 \times f_m$ at the lower 70% of the hillslope, $1.1 \times f_m$ at the sector ranging from 15 to 30% of the hillslope, and $1.5 \times f_m$ at the upper 15%, average macroporosity value was $f_m = 2.1$.
- Disturbed patterns of macroporosity and soils The spatial patterns of soils and macroporosity were flipped, i.e. calcaric regosols in the lower 80% and colluvisols

in the upper 20% of the hillslope, $0.6 \times f_m$ at the lower 70% of the hillslope, $1.1 \times f_m$ at the sector ranging from 15 to 30% of the hillslope, and $1.5 \times f_m$ at the upper 15%, average macroporosity value was $f_m = 2.1$.

– Sand on loess This completely different model structure consists of a sand layer of 1-m depth followed by calcaric regosols extending over the complete hillslope length, while macropores were neglected. The soil hydraulic parameters of the sand were taken from the pedotransfer function proposed by Carsel & Parrish (1988; see their Table 1).

After simulation the average catchment-scale soil saturation and the average catchment-scale matric potential were derived from the model output as outlined in equation (6). As can be seen in Fig. 14.5, illustrating the largest rainfall event (27 June 1994), as expected, the different model structures cause clear differences in runoff responses. Sand on top of the loess soil yields a retarded and reduced runoff response, which stems from subsurface storm flow on the loess horizon at 1 m depth. It is remarkable that the rearrangement, i.e. the flipping of the soil and macroporosity patterns, is sufficient to yield clearly different rainfall–runoff behaviour.

Figure 14.6 shows the time series of the catchment-scale average soil saturation (upper panel) and catchment-scale average matric potential, which result from the different model structures (lower panel). The time series derived from the landscape and process compatible model structure differ clearly from those derived from the remaining model structures. Major differences occur during strong rainfall events, e.g. on day 67 (27 June 1994), and persist for more than 100 days.

The time series of catchment-scale state variables (Fig. 14.6) demonstrate clearly and unambiguously that the effects of within-catchment heterogeneity of soils and macropores on soil moisture dynamics do not vanish when we move to the next higher scale. The time series of catchment-scale average soil moisture and matric potential derived from the landscape and process compatible model structure are physically consistent with a distributed set of observations taken inside the catchment, whereas those derived from the remaining model structures are inconsistent. These state variables are capable of reflecting and embedding within them the effects of the dominant within-catchment heterogeneities on the subsurface dynamics operating at the REW scale, and are physically consistent with information of within-catchment observations of ET, discharge and soil moisture.

Derivation of REW-scale Water Retention Functions

In this section we will introduce closure relations for catchment-scale average matric potential as a function of catchment-scale average water saturation, i.e. the catchment-scale average water retention curve, derived according to equations (12) and (13). By comparing different model structures we want to exemplify that different within-catchment patterns of soil and macroporosity yield different exponents in the catchment-scale average water retention function. To this end, the four following model structures were compared during a simulated catchment multi-step outflow experiment, as well as a simulated catchment-scale wetting experiment:

– Landscape and process compatible model structure This is the structure that yielded the predictions presented in the previous section, i.e. calcaric regosols in the upper 80% and colluvisols in the lower 20% of the hillslope (see Table 14.1

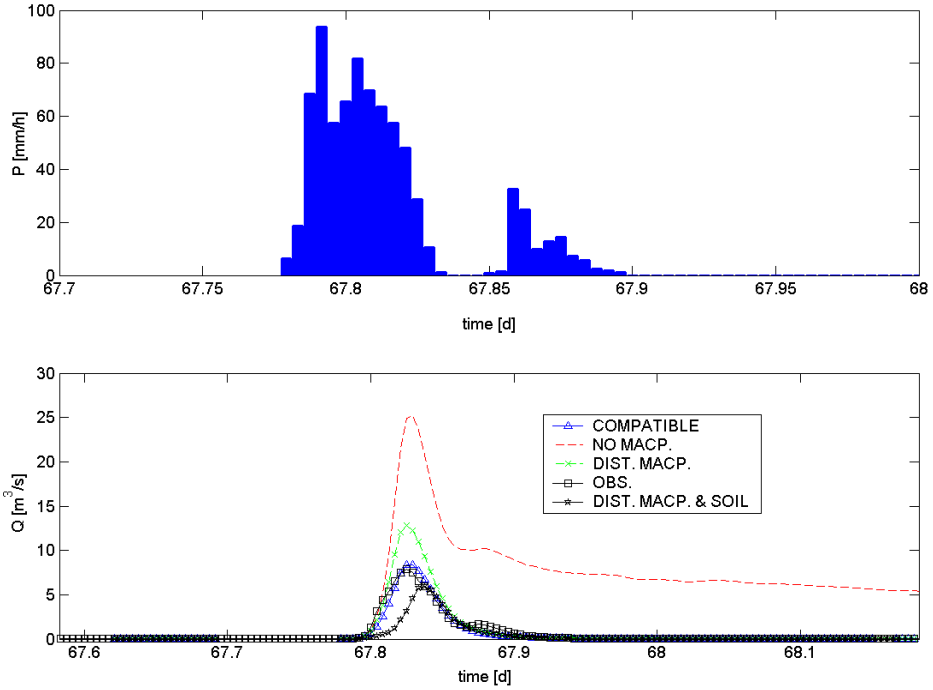

Fig. 14.5 *Differences in simulated discharge between different model structures shown through the example of the largest rainfall event on record (27 June 1994).*

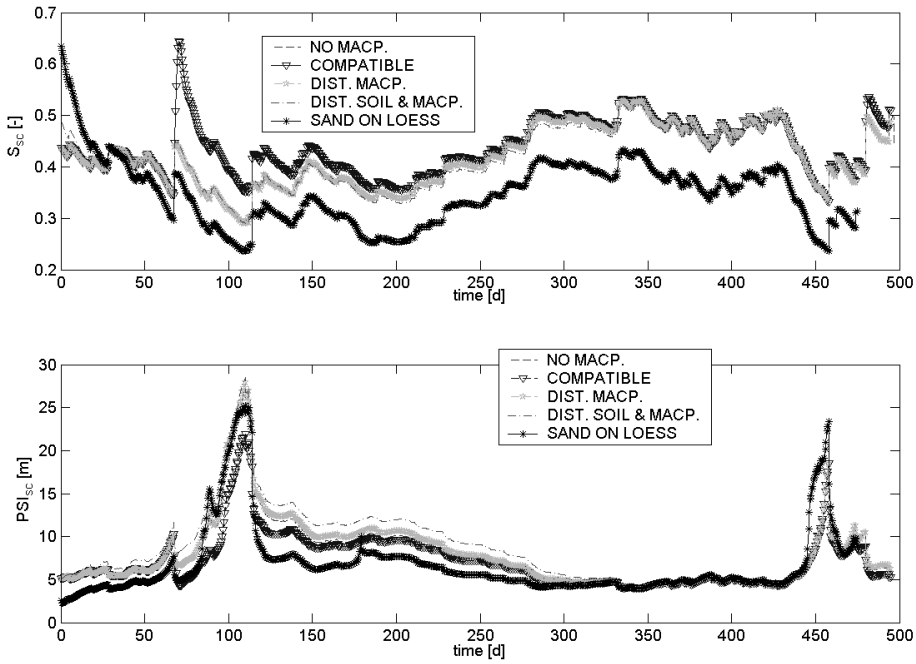

Fig. 14.6 *Average catchment-scale soil saturation (top) and average catchment-scale matric potential (bottom) computed according to equation (1) for the different model structures.*

for soil hydraulic parameters), deterministic macroporosity pattern with $0.6 \times f_m$ at the upper 70% of the hillslope, $1.1 \times f_m$ at the mid sector ranging from 70 to 85% of the hillslope, and $1.5 \times f_m$ at the lowest 85–100%, average macroporosity value was $f_m = 2.1$.

- Colluvisol model structure The entire hillslopes consists of colluvisol soils, the macroporosity pattern is the same as in the process consistent model structure.
- Calcaric regosol model structure The entire hillslope consists of calcaric regosols and the macroporosity pattern is the same as in the process consistent model structure.
- Sand on loess A sand layer of 1-m depth followed by calcaric regosols extend over the complete hillslope length, and macropores were neglected.

During the catchment-scale drying experiment, denoted in the following as the drying case, we started with an initially saturated catchment, and imposed an increasing suction as a function of time (Fig. 14.7 upper right panel) as the lower boundary condition to all hillslopes. Over the remaining upper, right, and left hillslope boundaries a zero-flux condition was imposed. During the catchment-scale wetting experiment, denoted in the following as the wetting case, we started at an initial soil water saturation of 0.05 for the entire catchment, and imposed a spatially homogeneous block of rain of 10 mm day^{-1} as the upper boundary condition (Fig. 14.7). Over the remaining lower, right, and left hillslope boundaries, a zero flux condition was imposed. In both the wetting and the drying cases the simulation period was 2 years.

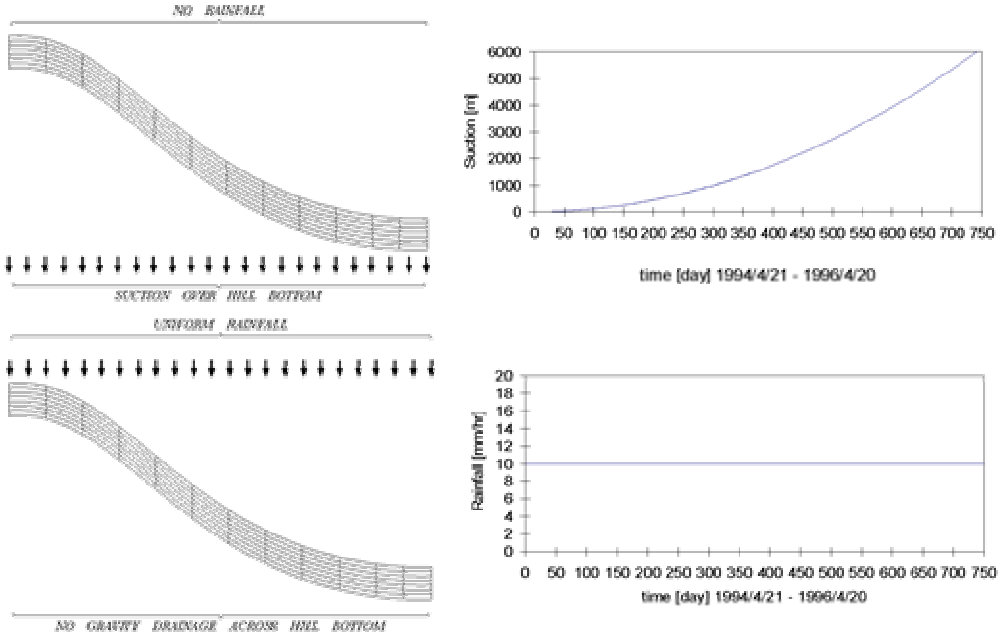

Fig. 14.7 *Suction as a function of time used (upper right panel) as lower boundary condition experiment during the simulated drainage experiment (upper left), at the other boundaries a zero-flux boundary condition was imposed. Constant rainfall rate (lower right panel) used as upper boundary conditions during the simulated wetting experiment (lower left panel), at the other boundaries a zero-flux boundary condition was imposed.*

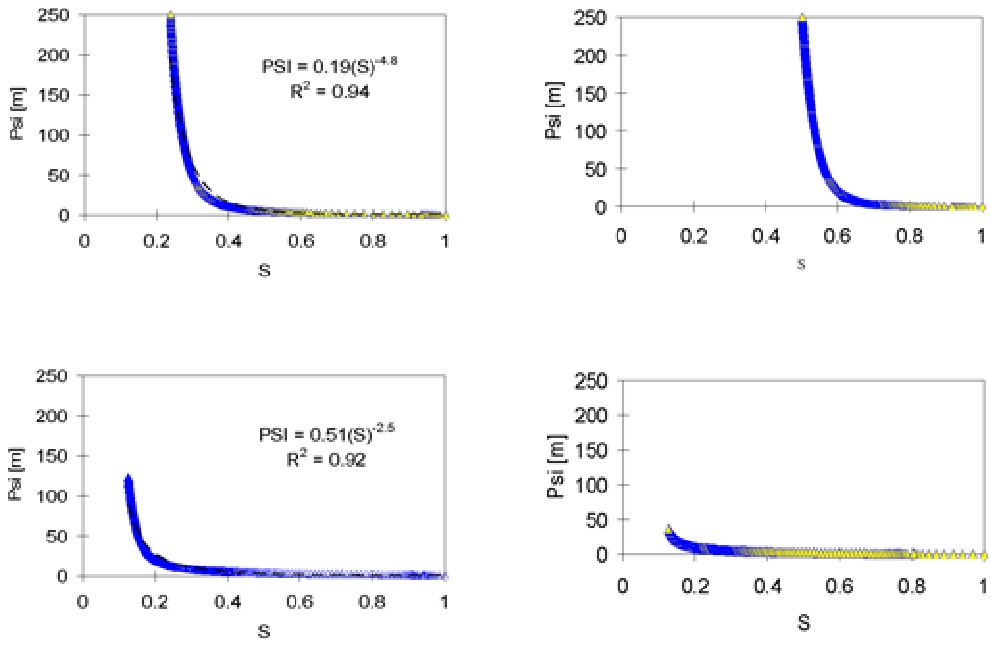

Fig. 14.8 *Average catchment-scale matric potential obtained in the drainage case plotted vs average catchment-scale soil saturation for the process consistent model structure (upper left), colluvisol model structure (upper right), calcaric regosol model structure (lower left) as well as sand on loess model structure.*

Figure 14.8 shows the average catchment-scale matric potential plotted against the average catchment-scale soil saturation, i.e. the catchment-scale average soil water retention curve, for the drying case. The catchment-scale water retention curve derived for the landscape and process consistent model structure differs clearly from those curves derived with other model structures. In general capillary forces on soil water are less intense, as in the case of the colluvisol model structure, but clearly stronger than in the case of sand on loess or calcaric regosols. If we fit a simple two parametric potential model as suggested in equation (13) to the experimental curves, we obtain reasonable fits. The stronger the capillary attraction, the larger is the absolute value of the β-exponent in equation (13). As can be seen from Fig. 14.9 the soil water retention curves obtained in the wetting experiment have a completely different shape. Apparently, there is strong hysteresis in the catchment-scale soil water retention function. In the case of uniform soil types on the slope the water retention curves have a linear shape. The spatial variability of soil types in the process consistent and the sand on loess model structure are likely the reason for the piecewise linear shape of the corresponding soil water retention curves (Fig. 14.9, top left and bottom right panel).

DISCUSSION AND OUTLOOK

The main findings of the present study may be condensed into the three following points:

– The representation of the dominant spatial patterns of soil heterogeneity and macroporosity in the process model CATFLOW, which are typical for this loess

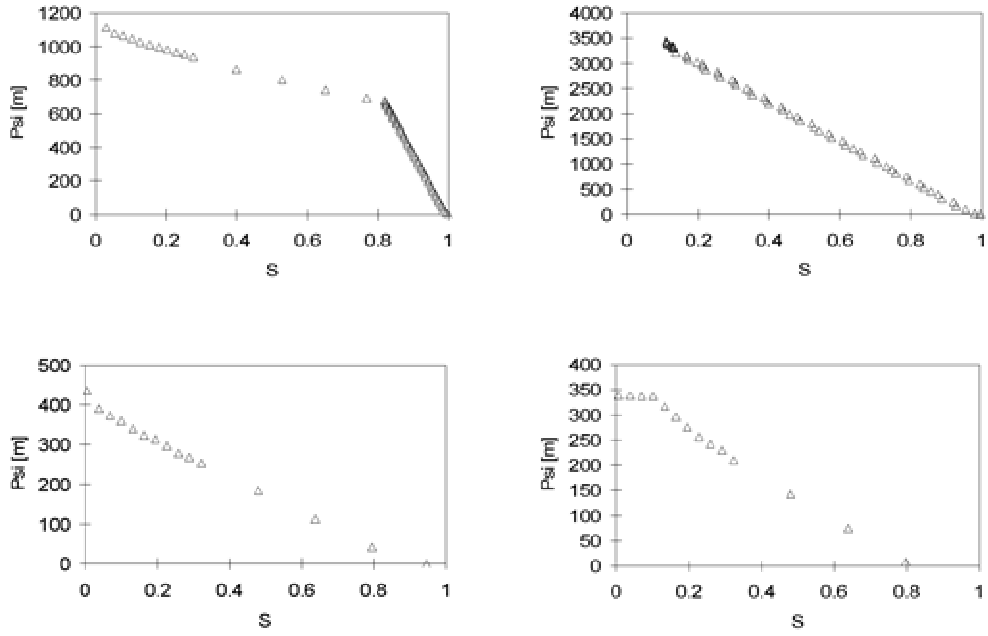

Fig. 14.9 *Average catchment-scale matric potential obtained in the wetting case plotted vs average catchment-scale soil saturation for the process consistent model structure (upper left panel), colluvisol model structure (upper right panel), calcaric regosol model structure (lower left panel) as well as sand on loess model structure. Please note the y-scales are different in different panels.*

area, was sufficient for explaining the major part of the observed discharge-, ET- and soil moisture dynamics in a typical catchment in a loess area of Germany. We want to stress in this context that it was not necessary to account for the exact soil catena and the small-scale variability of soil properties at the individual hillslopes. The model is landscape specific since it only accounts for dominant and typical heterogeneities, and process compatible, as it explains a large part of observed dynamics.

– We derived time series of catchment-scale average soil saturation and catchment-scale average matric potential by averaging the output of the landscape and process compatible model. The effects of within-catchment heterogeneity of soils and macropores on soil moisture dynamics do not vanish when we move to the next higher scale. The time series of catchment-scale average soil moisture and matric potential derived from the landscape and process compatible model structure are physically consistent with a distributed set of observations inside the catchment. These state variables are capable of reflecting and embedding within them the effects of the dominant within-catchment heterogeneities on subsurface dynamics at the REW-scale, and therefore suitable target data for testing subsurface components of mesoscale hydrological models. We consider this approach of dynamical upscaling much more appropriate for an upscaling of local observations than, for example, geo-statistical approaches, because it makes use of the maximum of current available physically-based process understanding as well

as understanding of the landscape by using a process models for interpolations/ aggregation.

– Furthermore, within simulated catchment-scale wetting and drying experiments, we derived catchment-scale soil water retention functions for different model structures. Different soil patterns within the catchment yielded, both in wetting and drying, clearly different soil water retention curves, and these differences were consistent with local scale soil pore spectra. Assuming a simple two parametric function for the soil water retention curve, different model structures yielded clearly different parameters. Coming back to the reasoning on the pattern–process paradigm, we consider the soil water retention curve derived from the landscape and process consistent model structure as a typical closure relation for describing the unsaturated zone mass balance equation in such a landscape. Because the model did account for the spatial patterns of soil and macropores that are typical for this loess area, which we call "general features of the place", but it neglects special details such as small-scale variability of soil and macropores or the presence of palaeo-soils, which make the Weiherbach catchment a unique individual catchment in the sense of Beven (2000).

As we used perturbation analysis in this paper, the presented methodology is similar to the approaches proposed by Duffy (1996) and Dagan (1986) to parameterize the first and second moment of tracer plumes in stochastic media in groundwater. However, contrary to Dagan's approach, our analysis is not based on hypothetical stochastic porous media with well behaved properties. It is based on the output and the parameter fields of a dynamic numerical model which has been shown to represent the typical spatial structures of the investigated loess area and to portray closely the behaviour of the hydrological system. This new method of dynamic upscaling may be generalized in the following sense: if representation for subsurface dynamics better than the Richards equation is available, these will be implemented in the dynamic model, but the uspcaling procedure will stay the same. The essential idea, i.e. to look for closure relations based on the averaged subsurface dynamics of a well-tested dynamical model, remains the same.

The necessary research steps in the future should:

(a) implement a root zone/upper soil layer in the REW theory as a separate zone as most soils in the world have some kind of layered structure;
(b) explore the effect of local-scale statistical variability of soil hydraulic properties;
(c) explore the dependency of derived closure relations on the grid resolution of the dynamical model;
(d) derive a catchment-scale soil hydraulic conductivity function and compare different ways for averaging hydraulic conductivity such as the harmonic, geometric and arithmetic mean;
(e) explore second order effects in derivation of a catchment-scale soil hydraulic conductivity function (compare equation (11));
(f) test the effect of different crop patterns and root depths for deriving closure relations to parameterize ET.

Although the present study is only the first step towards deriving typical closure relations for REW-based models, we believe that the approach presented is a suitable framework for this task as well as for deriving commensurate REW-scale state measures from small-scale observations. Due to the concept of the process pattern

paradigm and the "generality of places", in the sense that typical patterns and structures in a landscape cause a generic spectrum of hydrological processes, we believe that REW-based models using typical closure relations will, in the end, require less calibration compared to both the physically-based and conceptual hydrological models used at the present time.

References

Bárdossy, A. & Lehmann, W. (1995) Distribution of soil moisture in a small catchment, Part 1: Geostatistical Analysis. *J. Hydrol.* **206**, 1–15.

Beven, K. (1989) Changing ideas in hydrology—the case of physically based models. *J. Hydrol*. **105**, 157–172.

Beven, K. J. (2000) Uniqueness of place and process representations in hydrological modelling. *Hydrol. Earth System Sci.* **4**(2), 203–213.

Beven, K. & Freer, J. (2001) Equifinality, data assimilation, and data uncertainty estimation in mechanistic modelling of complex environmental systems using the GLUE methodology. *J. Hydrol*. **249**(1–4), 11–29.

Bronstert, A. & Plate, E. J. (1997) Modelling of runoff generation and soil moisture dynamics for hillslopes and micro catchments. *J. Hydrol*. **198**(1–4), 177–195.

Carsel, R. F. & Parrish, R. S. (1988) Development of joint probability distributions of soil water retention characteristics. *Water Resour. Res.* **24**(5), 755–769.

Dagan, G. (1986) Statistical theory of groundwater flow and transport: pore to laboratory, laboratory to formation and formation to regional scale. *Water Resour. Res*. **22**(9), 120–134.

Duffy, C. (1996) A two-state integral-balance model for soil moisture and groundwater dynamics in complex terrain. *Water Resour. Res.* **32**(8), 2421–2434.

Ehrmann, O. (1996) Regenwürmer in einigen südwestdeutschen Agrarlandschaften: Vorkommen, Entwicklung bei Nutzungsänderung und Auswirkung auf das Bodengefüge. *Hohenheimer Bodenkundliche Hefte Nr. 35*. University of Hohenheim, Stuttgart, Germany.

Flury, M. (1996) Experimental evidence of transport of pesticides through field soils—a review. *J. Environ. Qual.* **25**(1), 25–45.

Grayson, R. B. & Blöschl, G. (eds) (2000) *Spatial Patterns in Catchment Hydrology: Observations and Modeling*. Cambridge University Press, Cambridge, UK.

Grayson, R. B., Western, A. W., Chiew, F. H. S. & Blöschl, G. (1997) Preferred states in spatial soil moisture patterns: local and non-local controls. *Water Resour. Res.* **33**(12), 2897–2908.

Gerlinger, K. (1997) Erosionsprozesse auf Lößböden: Experimente und Modellierung. Dissertation at the Institute of Water Resources Planning and Rural Engineering, University of Karlsruhe, Germany.

Hundecha, Y. & Bárdossy, A. (2004) Modeling of the effect of landuse changes on the runoff generation of a river basin through parameter regionalization of a watershed model. *J. Hydrol*. **292**, 281–295.

Maurer, Th. (1997) Physikalisch begründete, zeitkontinuierliche Modellierung des Wassertransports in kleinen ländlichen Einzugsgebieten. *Mitteilungen des Instituts für Hydrologie und Wasserwirtschaft, Heft 61*. Universität Karlsruhe, Germany.

Mualem, Y. (1976) A new model for predicting the hydraulic conductivity of unsaturated porous media. *Water Resour. Res.* **12**, 513–522.

Refsgaard, J. C. & Storm, B. (1995) MIKE SHE. In: *Computer Models of Watershed Hydrology* (ed. by V. P. Singh), 809–846. Water Resources Publications, Highland Ranch, Colorado, USA.

Reggiani, P., Sivapalan, M. & Hassanizadeh, S. M. (1998) A unifying framework for watershed thermodynamics: balance equations for mass, momentum, energy and entropy and the second law of thermodynamics. *Adv. Water Resour.* **22**(4), 367–398.

Reggiani, P., Hassanizadeh, S. M., Sivapalan, M. & Gray W.G. (1999) A unifying framework for watershed thermodynamics: constitutive relationships. *Adv. Water Resour.* **23**(1), 15–39.

Schäfer, D. (1999) Bodenhydraulischen Funktionen eines Kleineinzugsgebiets—Vergleich und Bewertung unterschiedlicher Verfahren. Dissertation, Institute of Hydromechanics, University of Karlsruhe, Germany.

Simunek, J., Vogel, T. N. & van Genuchten, M. T. (1994) The SWMS-2D code for simulating water and solute transport in two dimensional variably saturated media – Version 1.2. *Research Report 132, US Salinity Lab., Agric. Res. Serv.* USDA, Riverside, California, USA.

Sivapalan, M., Takeuchi, K., Franks, S. W., Gupta, V. K., Karambiri, H., Lakshmi, V., Liang, X., McDonnell, J. J., Mendiondo, E. M., O'Connel, P. E., Oki, T., Pomeroy, J. W., Schertzer, D., Uhlenbrook, S. & Zehe, E. (2003a) IAHS decade on Predictions of Ungauged Basins (PUB): Shaping an exciting future for the hydrological sciences. *Hydrol. Sci. J.* **48**(6), 857–879.

Sivapalan, M., Blöschl, G., Zhang, L. & Vertessy, R. (2003b) Downward approach to hydrological prediction. *Hydrol. Processes* **17**, 2101–2111. DOI 10.1002/hyp.1425.

Turner, M. G. (1989) Landscape ecology: the effect of pattern on process. *Annual Review of Ecology and Systematics* **20**, 171–197.

Turner, M. G., Gardner, R. H. *et al.* (2001) *Landscape Ecology in Theory and Practice—Pattern and Process*. Springer, New York, USA.

van Genuchten, M. T. (1980) A closed-form equation for predicting the hydraulic conductivity of unsaturated soils. *Soil Sci. Soc. Am. J.* **44**, 892–898.

Watt, A. S. (1947) Pattern and process in the plant community. *J. Ecol.* **35**(1), 1–22.

Western, A. W. & Grayson, R. B. (1998) The Tarrawarra data set: soil moisture patterns, soil characteristics and hydrological flux measurements. *Water Resour. Res.* **34**(10), 2765–2768.

Wood, E. F. (1976) An analysis of the effects of parameter uncertainty in deterministic hydrologic models, *Water Resour. Res.* **12**(5), 925–932.

Zehe, E. (1999) Stofftransport in der ungesättigten Bodenzone auf verschiedenen Skalen. Dissertation. University of Karlsruhe, Germany.

Zehe, E. & Blöschl, G. (2004) Predictability of hydrologic response at the plot and catchment scales – the role of initial conditions. *Water Resour. Res.* **40**, W10202, DOI 10.1029/2003WR002869.

Zehe, E. & Flühler, H. (2001) Slope scale variation of flow patterns in soil profiles. *J. Hydrol.* **247**(1–2), 116–132.

Zehe, E., Maurer, Th., Ihringer, J. & Plate, E. (2001) Modelling water flow and mass transport in a loess catchment. *Phys. & Chem. of Earth*, Part B **26** (7–8), 487–507.

Zurmühl, T. & Durner, W. (1996) Modelling transient water flow and solute transport in a biporous soil. *Water Resour. Res.* **32**(4), 819–829.